Los Alamos
NATIONAL LABORATORY
EST. 1943

LA-UR-21-22400
Approved for public release; distribution is unlimited.

Title: Particle-In-Cell Computer Simulations of Beam Spill in the Scorpius Injector

Author(s): Burris-Mog, Trevor John
Ekdahl, Carl August Jr.
Stem, Will

Intended for: Technical Note for the ASD Scorpius Project

Issued: 2021-03-10

Disclaimer:
Los Alamos National Laboratory, an affirmative action/equal opportunity employer, is operated by Triad National Security, LLC for the National Nuclear Security Administration of U.S. Department of Energy under contract 89233218CNA000001. By approving this article, the publisher recognizes that the U.S. Government retains nonexclusive, royalty-free license to publish or reproduce the published form of this contribution, or to allow others to do so, for U.S. Government purposes. Los Alamos National Laboratory requests that the publisher identify this article as work performed under the auspices of the U.S. Department of Energy. Los Alamos National Laboratory strongly supports academic freedom and a researcher's right to publish; as an institution, however, the Laboratory does not endorse the viewpoint of a publication or guarantee its technical correctness.

Particle-In-Cell Computer Simulations of Beam Spill in the Scorpius Injector

Trevor Burris-Mog [a], Carl Ekdahl [b] and Will Stem [c]

[a] Nevada National Security Site
[b] Los Alamos National Laboratory
[c] Lawrence Livermore National Laboratory

March 2021

Abstract

Computer simulations of beam transport in the Scorpius injector were performed using the particle-in-cell computer code LSP. The simulations were used to predict spot size growth due to electron stimulated emission of ions from beam spill on the anode stalk and the entrance transport region [1, 2].

The Injector

The Scorpius injector is being designed to provide multi-pulse capabilities for flash-radiography applications at the U1a Facility. Forty-two IVA cells will be driven by solid state pulse power and supply a 2 Mega-volt electric potential across the A-K gap in a 1:1 push-pull ratio. The 2 MeV electron beam will have a current of 1.5 kilo-amps with expected rise- and fall-times in the 15 to 25 nanosecond range.

A smooth, well controlled logistics function was initially used in the beam transport simulations, however it was decided that a measured waveform from the TM-05 pulser would have rise- and fall-times that will be more representative of the waveform from the final pulser design. The TM-05 waveform shown in Figure 1 was modified as follows:

- The steady-state emission time was reduced from 120 nanoseconds to 50 nanoseconds.
- We assumed the energy variation during steady-state will be reduced as both technical maturation and our understanding of pulse modulation continue. Because of this assumption, the top of the measured pulse was flattened.

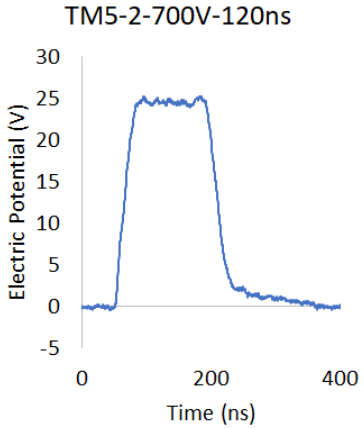

Figure 1: Measured TM-05 waveform from file TM5-2-700V-120ns-4pulse-500nsPerios-Vpulser used to generate the waveform in Figure 2.

- The pulse was repeated to create four pulses separated by 200 ns.
- Figure 2 shows the final result.

The distance from the cathode face to the first accelerator cell gap was 8.8 meters, and the magnetic transport fields were tuned to transport the steady-state electron beam to the accelerator. The space charge limited emission results in the head and tail of the electron beam having lower energy and lower current than that of the steady-state portion of the beam, which makes the head and tail intrinsically mismatched and leads to beam spill on the anode stalk and beam Entrance Transport Region (ETR). Figure 3 shows the transport and corresponding beam spill of the electrons during the rise of the beam pulse and the beam transport during the steady state (matched) portion of the beam pulse.

The solid line in Figure 4 shows the beam current at the cathode (z = 0), while the dashed line shows the beam current at z = 724 centimeters downstream from the cathode. The difference between the two plots is a result of the beam spill.

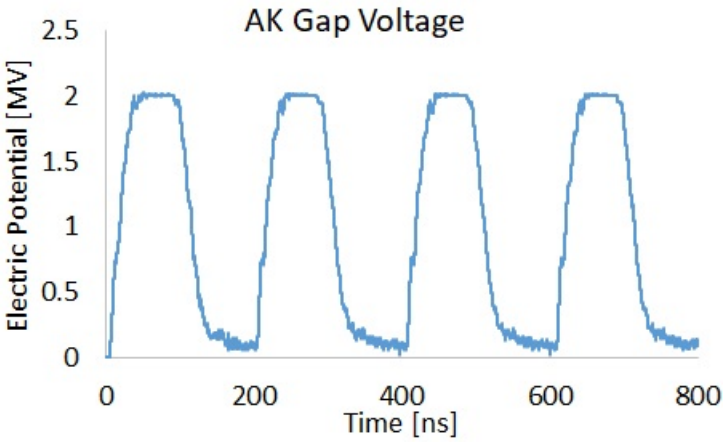

Figure 2: Waveform used in the computer simulation for the A-K gap electric potential.

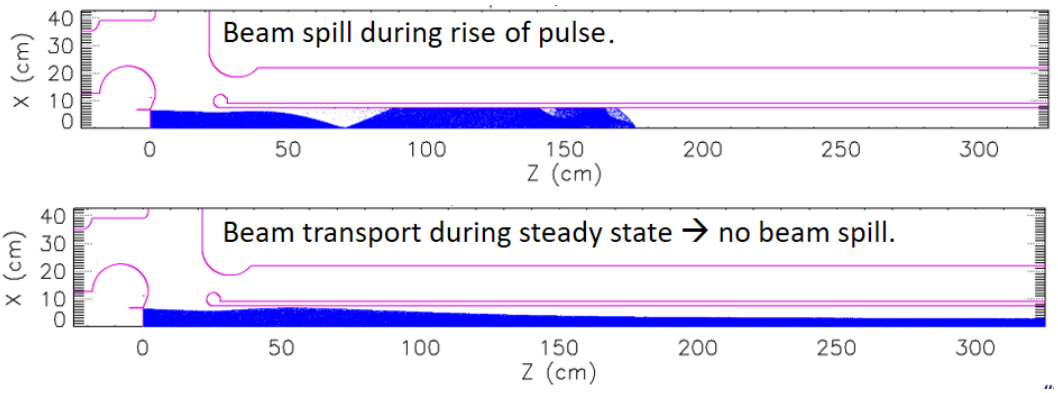

Figure 3: **Top** - Beam transport of the head of the electron beam, which has lower energies and lower currents compared to the steady state portion of the beam. **Bottom** - Beam transport of the 1.5 kA, 2 MeV (steady-state) the electron beam.

Stimulated Emission in LSP

LSP has the capability to simulate electron stimulated emission of ions from a surface. As with any computer simulation, there are limitations. Although the stimulated emission cross-section is dependent on the energy of the incident electron, the computer model only accepted a single, user entered value. Rudd's model [3] provided a theoretical calculation of the energy dependent cross-sections, and an approximate fit to Rudd's model provided an easy to use estimate of the theory. The number of electrons per energy bin were extracted and then converted to the number of electrons per cross-section bin. The average cross-section was found to be 7.1 x 10^{-19} cm^2, Figure 5, which was the single value used in our simulations.

The second limitation in our computer simulation was that only one species could be desorbed at a time per area. The computer model was able to add layers of different species to the surfaces of objects, but the desorption of each layer occurred in sequence, one layer (and therefore, one species) at a time. This required the first layer to be depleted before the next layer could begin to desorb.

Because the desorption of each layer of species occurred sequentially instead of together, it was decided that the computer model should bound the problem by simulated

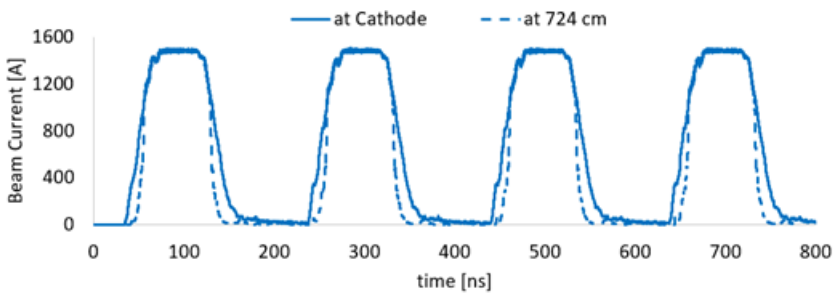

Figure 4: Electron beam current (solid line) at the cathode surface and (dashed line) at 724 cm downstream from the cathode surface.

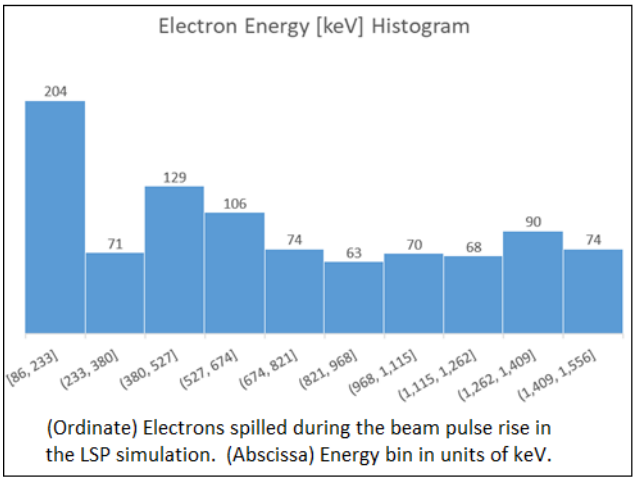

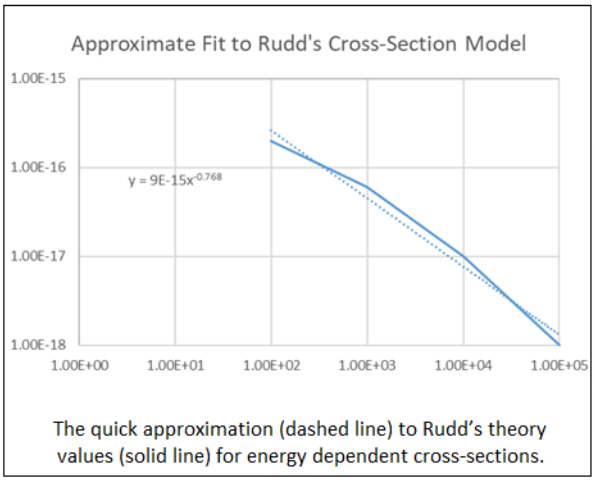

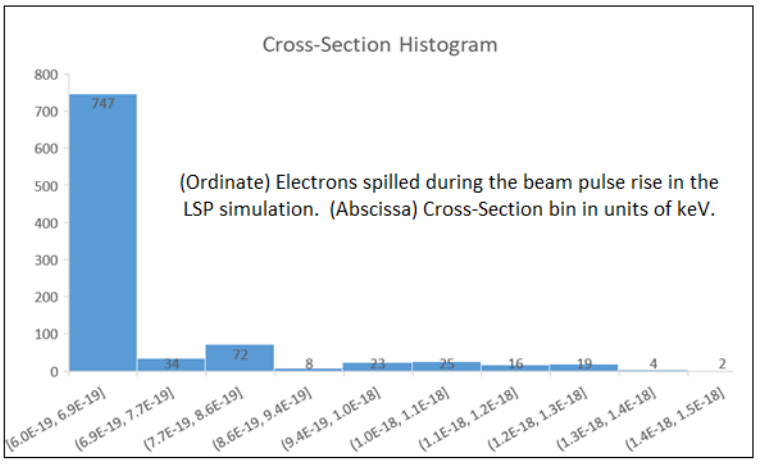

Figure 5:

the effects of a singe fast ion species (protons) and then repeat the simulations with a slow ion species (singly ionized water).

Beam Transport

Beam transport results are shown in Figures 6-13, while the effect on the RMS radius at z = 724 cm downstream from the cathode shown in Figure 14. At 724 cm, the electron beam has zero convergence. Since the electron beam also has zero convergence as it enters the final focus, these become point-to-point, parallel-to-parallel images. See [1, 2] for further reading.

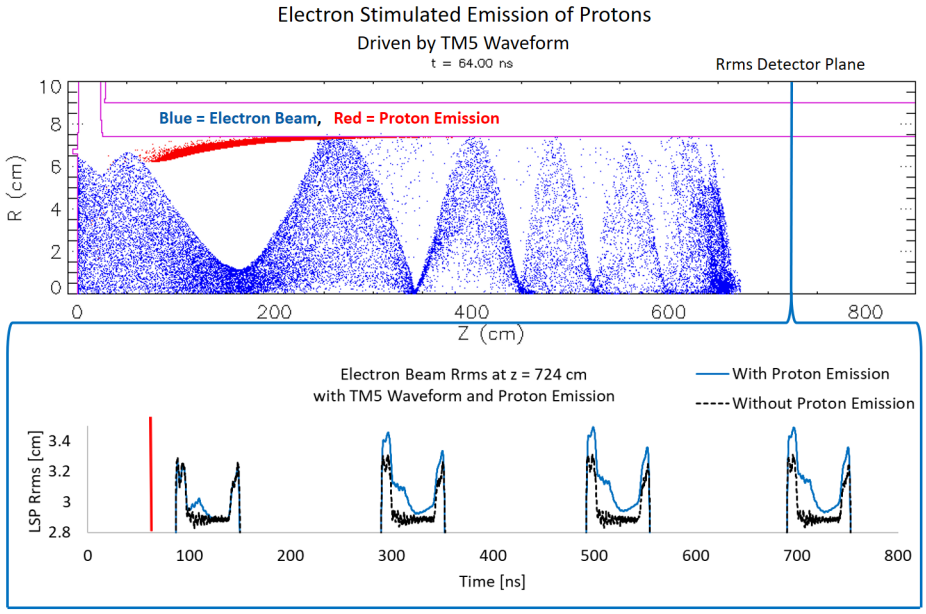

Figure 6: **Top** - Beam transport of electrons (blue) and protons (red) at 64 nanoseconds. **Bottom** - Beam current as a function of time for beam transport of electrons with (blue line) and without (black dashed line) stimulated emission.

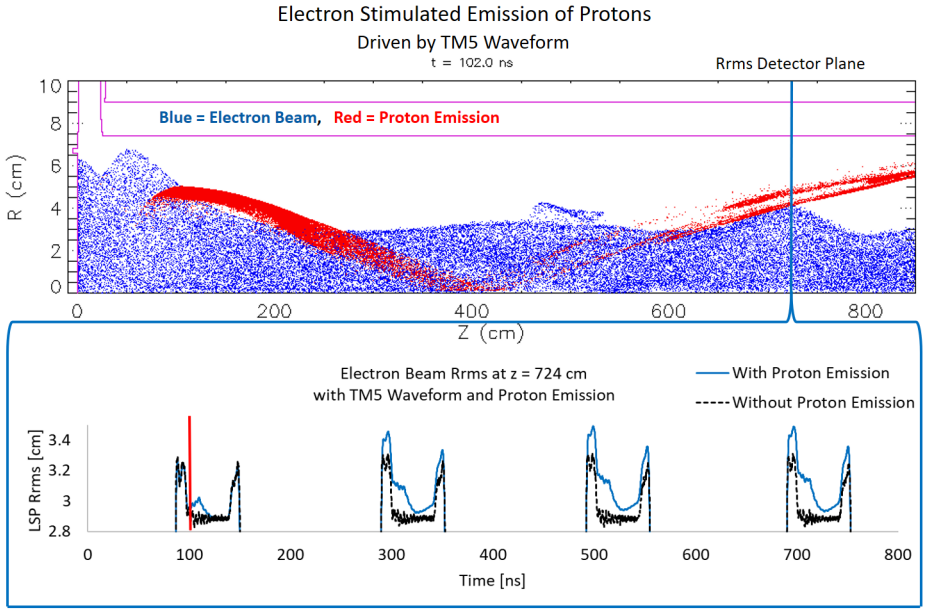

Figure 7: **Top** - Beam transport of electrons (blue) and protons (red) at 102 nanoseconds. **Bottom** - Beam current as a function of time for beam transport of electrons with (blue line) and without (black dashed line) stimulated emission.

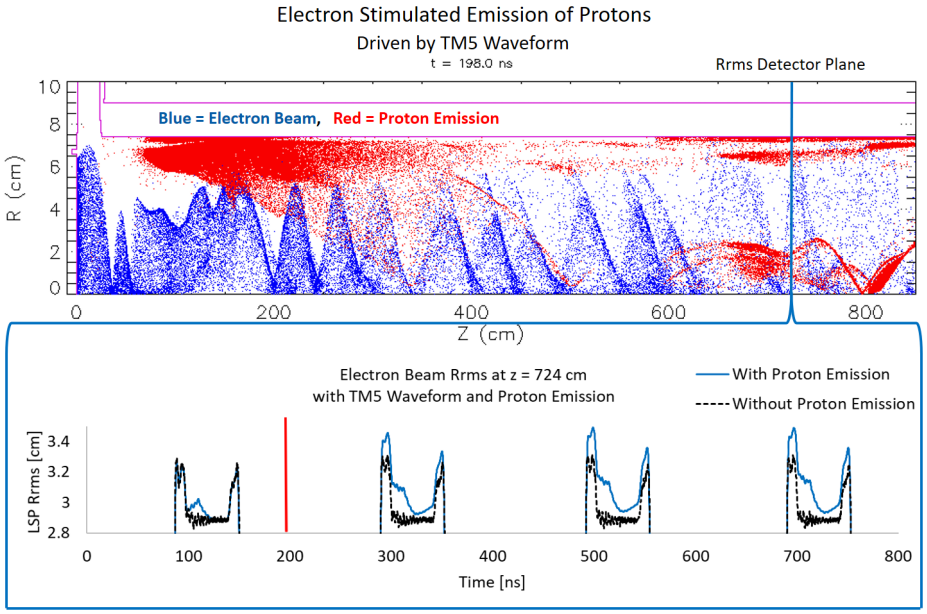

Figure 8: **Top** - Beam transport of electrons (blue) and protons (red) at 198 nanoseconds. **Bottom** - Beam current as a function of time for beam transport of electrons with (blue line) and without (black dashed line) stimulated emission.

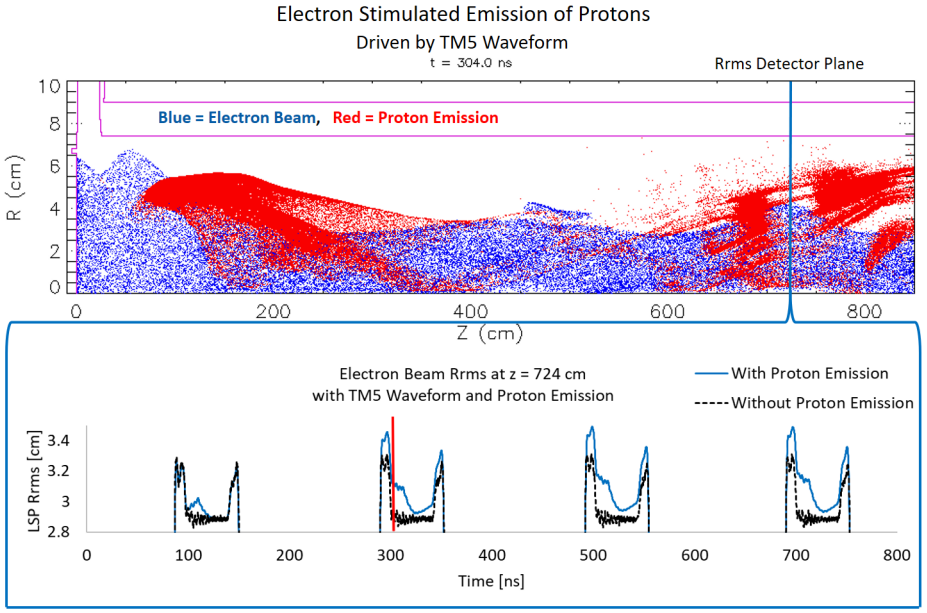

Figure 9: **Top** - Beam transport of electrons (blue) and protons (red) at 304 nanoseconds. **Bottom** - Beam current as a function of time for beam transport of electrons with (blue line) and without (black dashed line) stimulated emission.

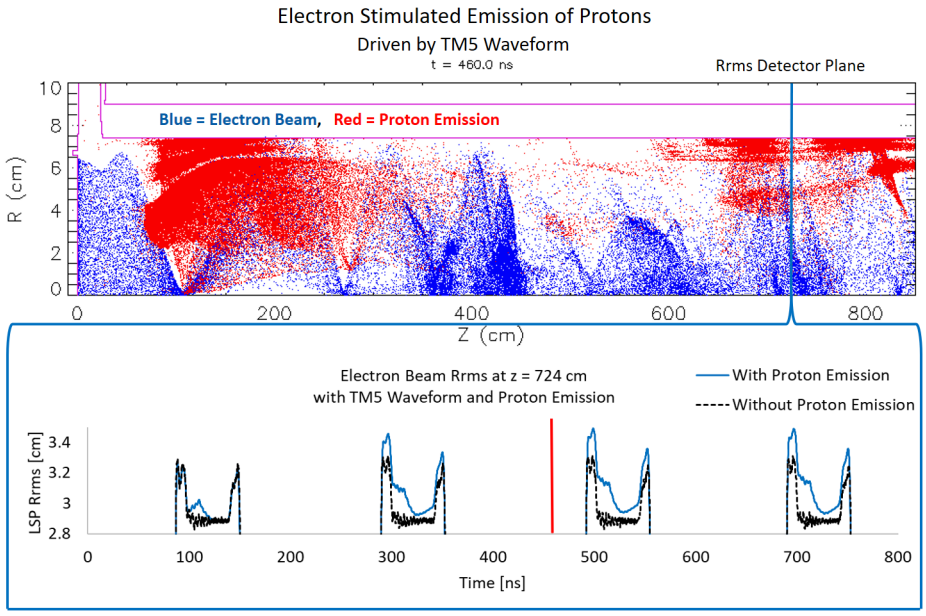

Figure 10: **Top** - Beam transport of electrons (blue) and protons (red) at 460 nanoseconds. **Bottom** - Beam current as a function of time for beam transport of electrons with (blue line) and without (black dashed line) stimulated emission.

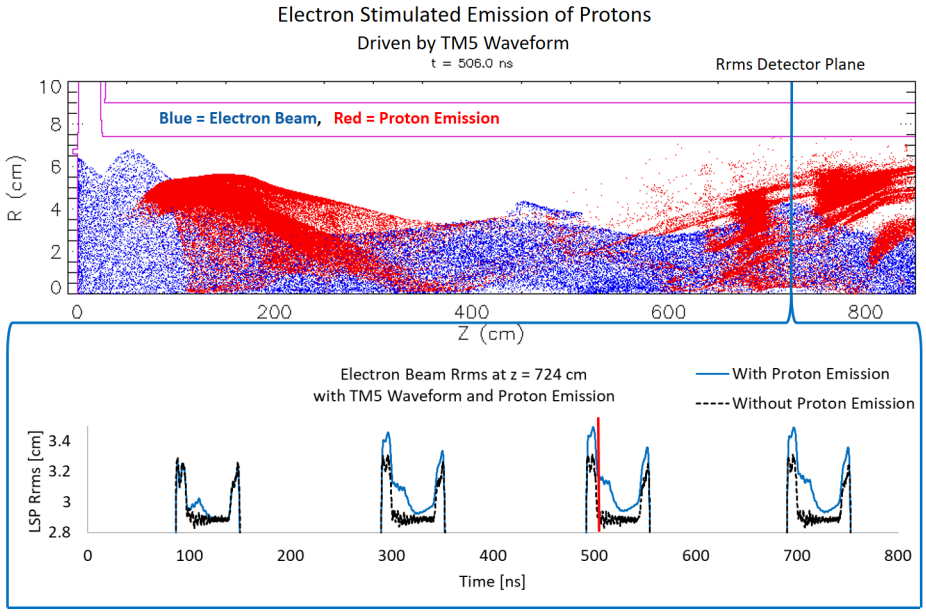

Figure 11: **Top** - Beam transport of electrons (blue) and protons (red) at 506 nanoseconds. **Bottom** - Beam current as a function of time for beam transport of electrons with (blue line) and without (black dashed line) stimulated emission.

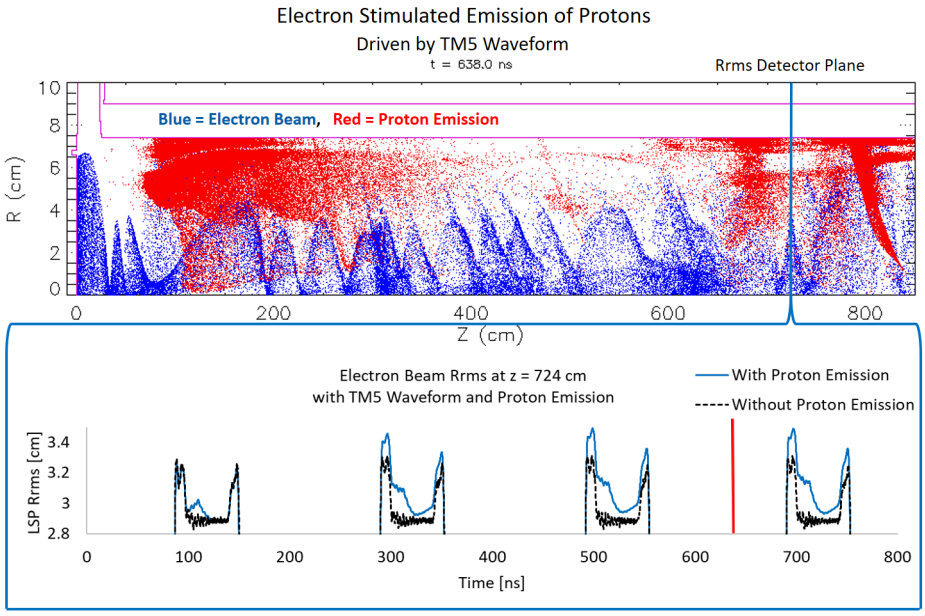

Figure 12: **Top** - Beam transport of electrons (blue) and protons (red) at 638 nanoseconds. **Bottom** - Beam current as a function of time for beam transport of electrons with (blue line) and without (black dashed line) stimulated emission.

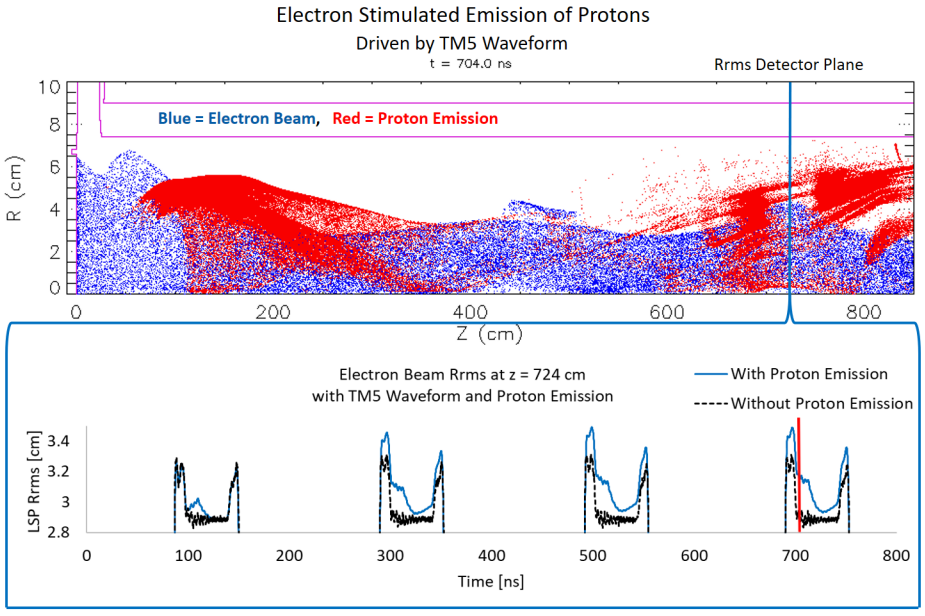

Figure 13: **Top** - Beam transport of electrons (blue) and protons (red) at 704 nanoseconds. **Bottom** - Beam current as a function of time for beam transport of electrons with (blue line) and without (black dashed line) stimulated emission.

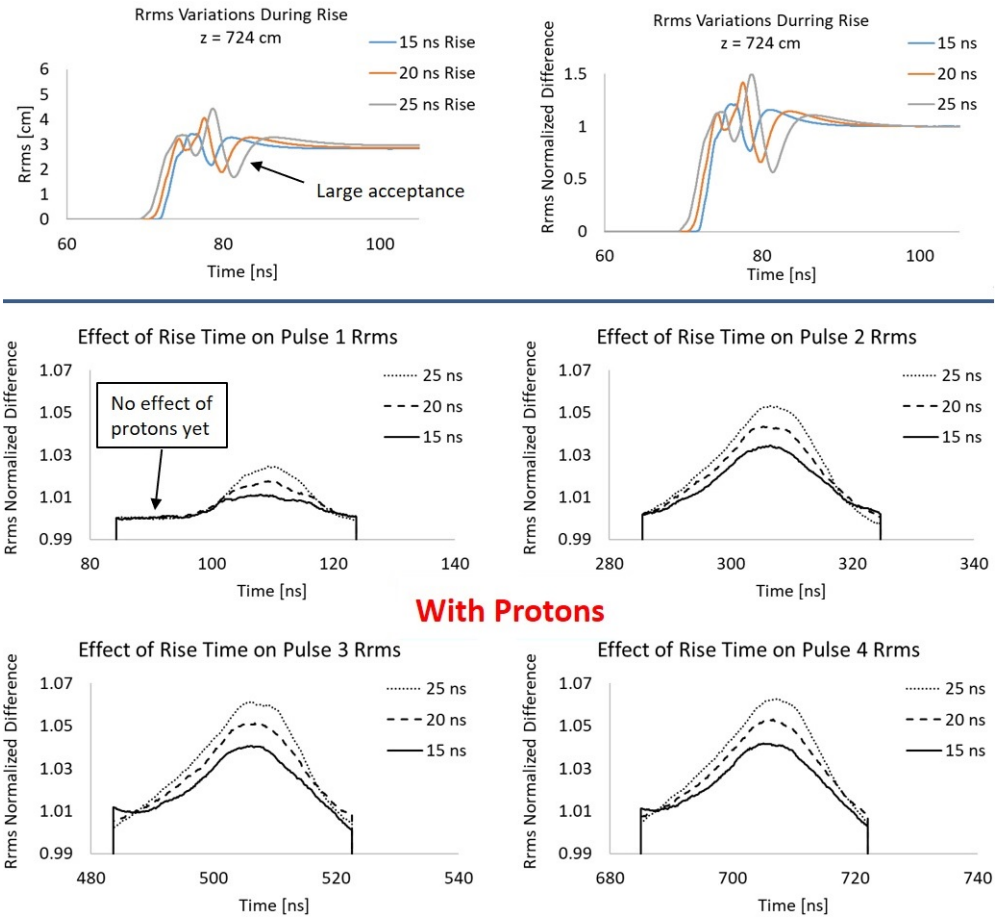

Figure 14: **Top Left** - RMS of the beam radius at z = 724 cm downstream from the cathode for 15, 20 and 25 nanosecond rise times without stimulated emission. **Top Right** - Normalized Differences of the RMS beam radius at z = 724 cm without stimulated emission. **Bottom** - Normalized Differences of the RMS beam radius at z = 724 cm with stimulated emission of protons for four 50 ns pulses separated by 200 ns.

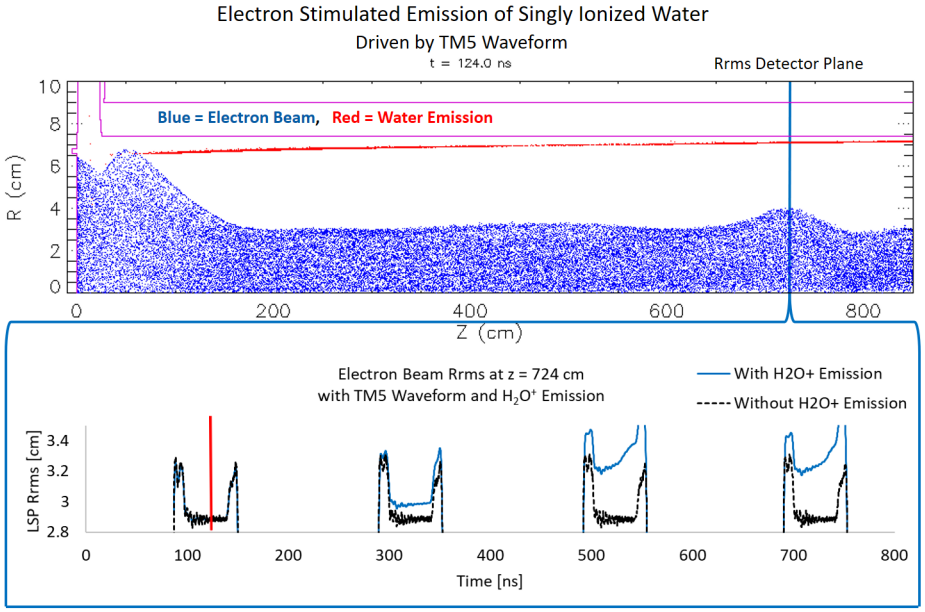

Figure 15: **Top** - Beam transport of electrons (blue) and singly ionized water (red) at 124 nanoseconds. **Bottom** - Beam current as a function of time for beam transport of electrons with (blue line) and without (black dashed line) stimulated emission.

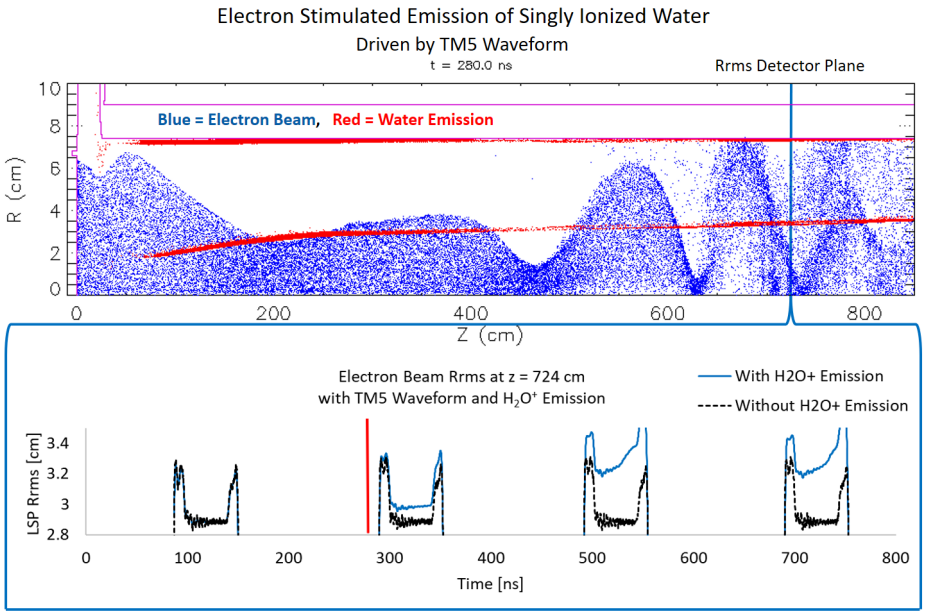

Figure 16: **Top** - Beam transport of electrons (blue) and singly ionized water (red) at 280 nanoseconds. **Bottom** - Beam current as a function of time for beam transport of electrons with (blue line) and without (black dashed line) stimulated emission.

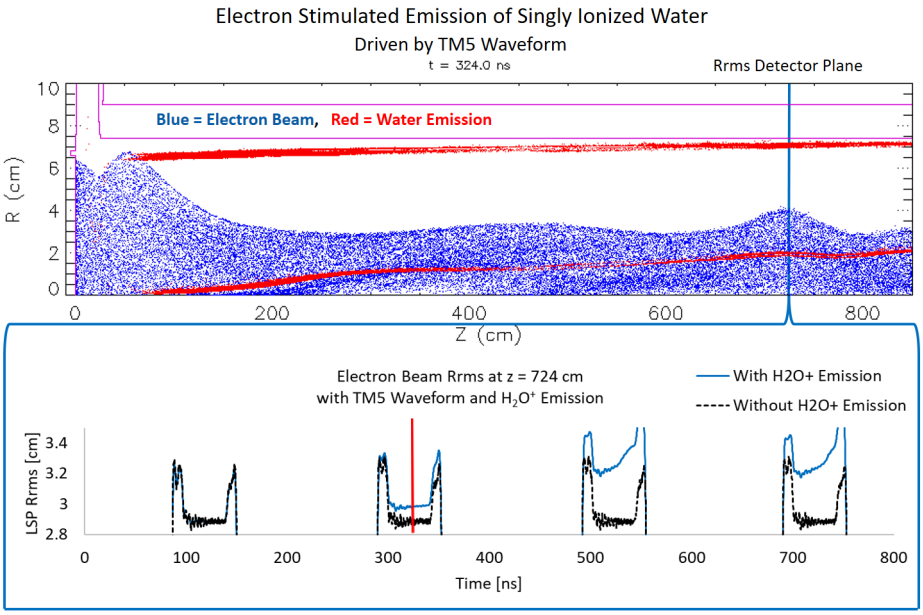

Figure 17: **Top** - Beam transport of electrons (blue) and singly ionized water (red) at 324 nanoseconds. **Bottom** - Beam current as a function of time for beam transport of electrons with (blue line) and without (black dashed line) stimulated emission.

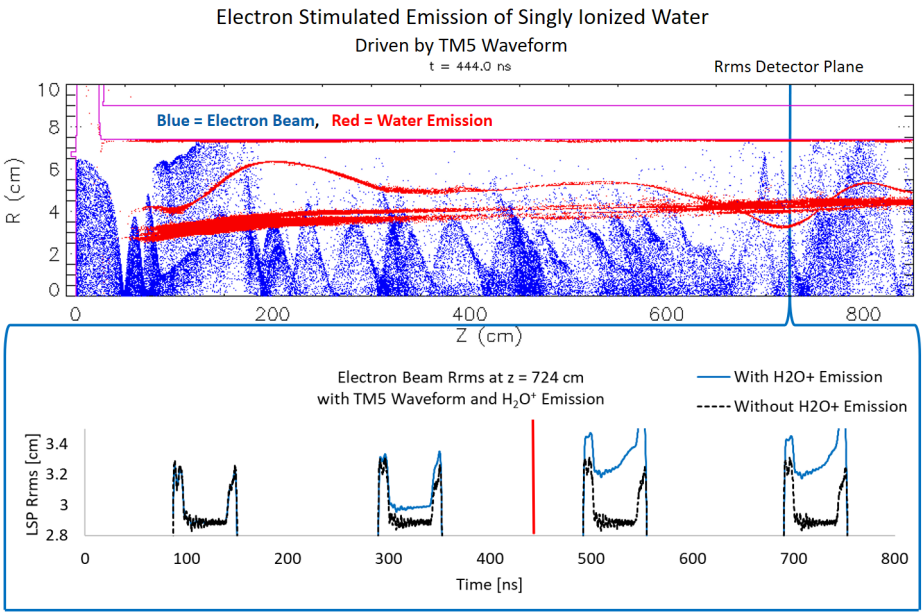

Figure 18: **Top** - Beam transport of electrons (blue) and singly ionized water (red) at 444 nanoseconds. **Bottom** - Beam current as a function of time for beam transport of electrons with (blue line) and without (black dashed line) stimulated emission.

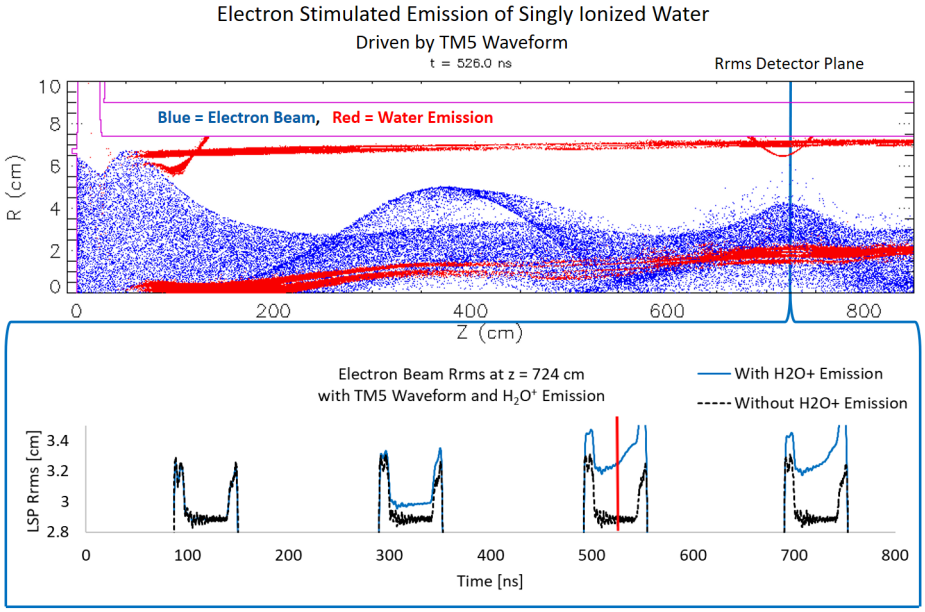

Figure 19: **Top** - Beam transport of electrons (blue) and singly ionized water (red) at 526 nanoseconds. **Bottom** - Beam current as a function of time for beam transport of electrons with (blue line) and without (black dashed line) stimulated emission.

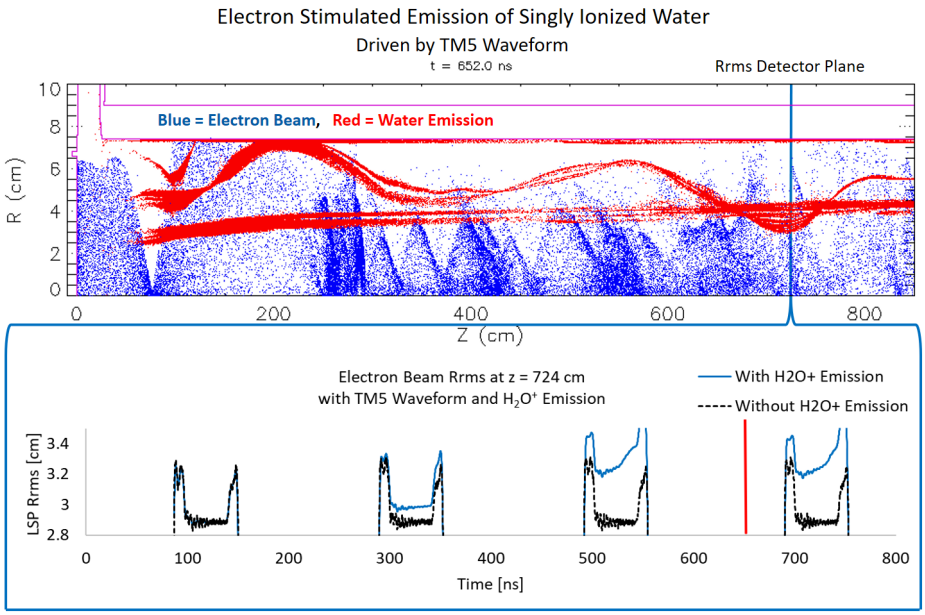

Figure 20: **Top** - Beam transport of electrons (blue) and singly ionized water (red) at 652 nanoseconds. **Bottom** - Beam current as a function of time for beam transport of electrons with (blue line) and without (black dashed line) stimulated emission.

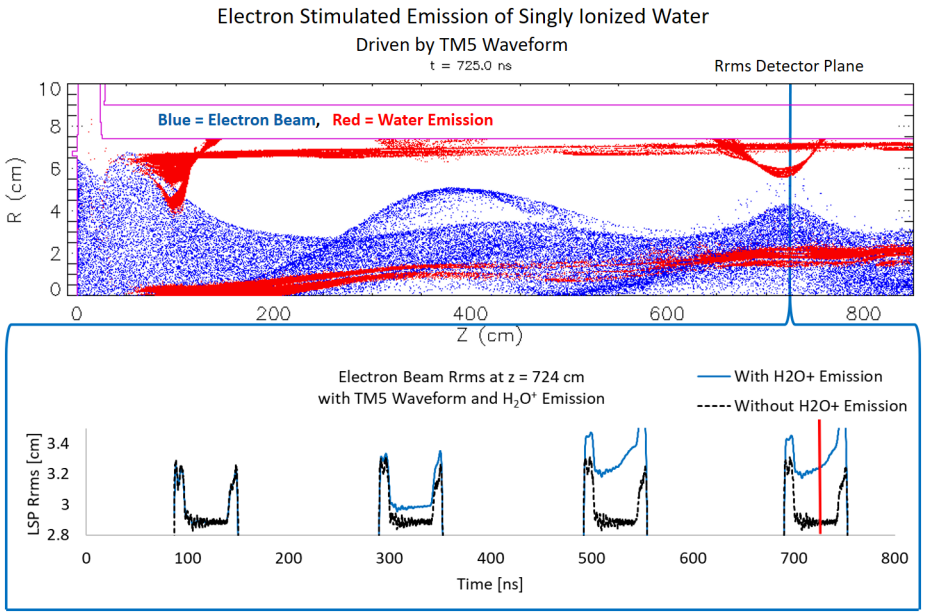

Figure 21: **Top** - Beam transport of electrons (blue) and singly ionized water (red) at 725 nanoseconds. **Bottom** - Beam current as a function of time for beam transport of electrons with (blue line) and without (black dashed line) stimulated emission.

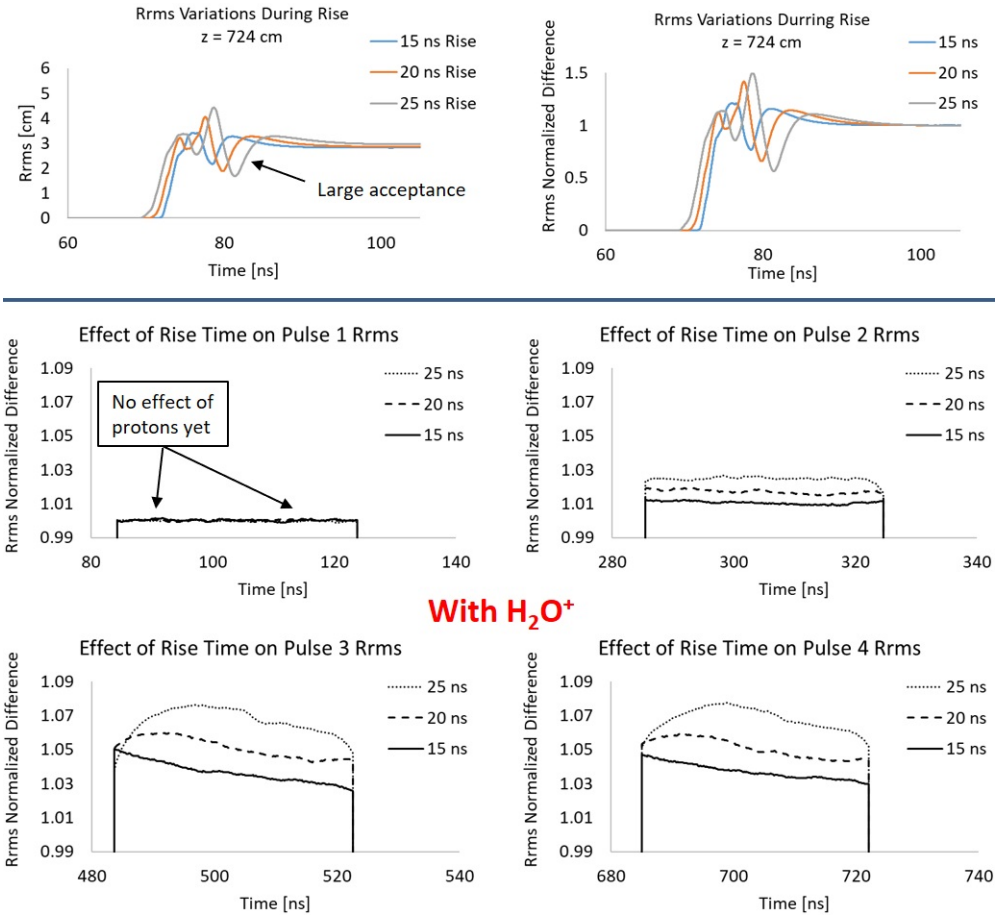

Figure 22: **Top Left** - RMS of the beam radius at z = 724 cm downstream from the cathode for 15, 20 and 25 nanosecond rise times without stimulated emission. **Top Right** - Normalized Differences of the RMS beam radius at z = 724 cm without stimulated emission. **Bottom** - Normalized Differences of the RMS beam radius at z = 724 cm with stimulated emission of singly ionized water for four 50 ns pulses separated by 200 ns.

References

[1] Carl Ekdahl. Spot-size enlargement due to injector beam spill. *Scorpius Technical Note (LA-UR-21-21103)*, February 2021.

[2] Carl Ekdahl, Trevor Burris, and Will Stem. Beam spill in downstream transport due to injector faults. *Scorpius Technical Note (LA-UR-21-20772)*, February 2021.

[3] Ianik Plante and Francis A Cucinotta. Cross sections for the interactions of 1 eV–100 MeV electrons in liquid water and application to monte-carlo simulation of HZE radiation tracks. *New Journal of Physics*, 11(6):063047, jun 2009.